Low-order feedforward controllers: Optimal performance and practical considerations

Hast, Martin; Hägglund, Tore

Published in:
Journal of Process Control

DOI:
10.1016/j.jprocont.2014.06.016

2014

Low-Order Feedforward Controllers: Optimal Performance and Practical Considerations

Martin Hast*, Tore Hägglund

Department of Automatic Control, Lund University, Box 118, SE-221 00 Lund, Sweden

Abstract

Feedforward control from measurable disturbances can significantly improve the performance in control loops. However, tuning rules for such controllers are scarce. In this paper design rules for how to choose optimal low-order feedforward controller parameter are presented. The parameters are chosen so that the integrated squared error, when the system is subject to a step disturbance, is minimized. The approach utilizes a controller structure that decouples the feedforward and the feedback controller. The optimal controller can suffer from undesirable high-frequency noise characteristics and tuning methods for how to filter the control signal are also provided. For scenarios where perfect disturbance attenuation in theory is achievable but where noise-filtering is needed, the concept of precompensation is introduced as a way to shift the controller time-delay to compensate for the low-pass filtering.

Keywords: Feedforward control, controller design, optimal control, load-disturbance rejection, filtering.

1. Introduction

Feedforward is an efficient way to reduce control errors both for reference tracking and disturbance rejection, given that the disturbances acting on the system are measurable. This paper addresses tuning of feedforward controllers for rejection of measurable disturbances. The use of feedforward alone often cannot eliminate the disturbance completely and it is therefore often used along with feedback control.

For design of PID-controllers there exists a large number of tuning methods for choosing the control parameters, see e.g., [2, 12, 15, 18]. However, there is a lack of methods for how to tune feedforward controllers in order to efficiently attenuate disturbances.

*Corresponding author. Tel.: +46 46 222 97 45.

Email addresses: martin.hast@control.lth.se (Martin Hast), tore.hagglund@control.lth.se (Tore Hägglund)

The design of low-order feedforward controllers has previously been addressed by e.g., [7, 8, 10, 13]. In [10] an iterative design procedure is proposed that minimizes a system norm in the frequency domain, taking the feedback controller into account. In [7] simple tuning rules for feedforward controllers, that reduces the integrated absolute error, are provided. An overview of loworder feedforward from both references and load disturbances are discussed in [16].

In [4] a feedforward structure that separates the feedback and feedforward control design, was presented. This idea has been adopted in this paper and justifies that the designed controller, while optimal in the open-loop case, gives good performance when used in conjunction with feedback control. This structure makes use of the same process models that are used for the design of the feedforward controller. The structure has similarities with Internal Model Control, IMC, see [6]. Robust feedforward design within the IMC framework was addressed by [17]. The method of subtracting the feedforward response from the controller input is common when improving system response from reference signals, cf. [3].

This paper presents an analytic solution to the problem of designing a feedforward lead-lag filter which minimizes the integrated square error when the system is subjected to a measurable step disturbance. The design rules are derived for stable process with dynamics described by first-order plants with dead time, (FOTD). The paper also discusses how a feedforward controller should be filtered in order to reduce the effect of measurement noise and aggressive controller actions. Lastly, tuning rules for reducing the control signal activity by precompensation is presented.

2. Feedforward control

Feedforward control from measurable disturbances has usually been treated and solved as an open-loop problem. For a system described by Fig. 1 the transfer function from the measurable disturbance d to system output y is

$$G_{\mathrm{o}}(s) = P_d(s) - P_u(s)F(s). \tag{1}$$

In order to completely eliminate the effect of the disturbance d the feedforward controller should be chosen as

$$F(s) = \frac{P_d(s)}{P_u(s)}. \tag{2}$$

This controller is not realizable for instance if the time-delay in $P_u(s)$ is longer than that of $P_d(s)$ or if $P_u(s)$ has zeros in the right-half plane. If the controller is realizable it might give rise to larger control signals than what is desirable. Common remedies for this is to use a low-order approximation of (2) or even just the static gain [3].

Due to model errors, uncertainties and other disturbances than the measurable acting on the system, feedforward controllers are often used together with

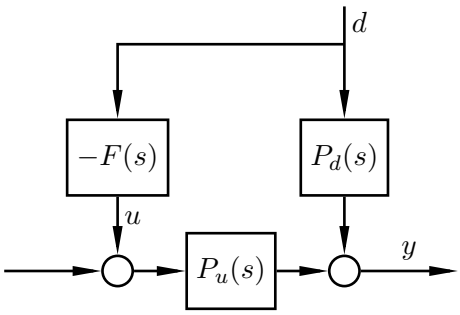

Figure 1: Open-loop structure for disturbance rejection using feedforward control.

feedback controllers. By combining a feedforward controller with an output feedback controller with the structure in Fig. 2 the transfer function from d to y becomes

$$G_{yd}(s) = \frac{P_d(s) - P_u(s)F(s)}{1 + P_u(s)C(s)}. \tag{3}$$

Using this structure, and the controller given by (2), perfect disturbance rejection is possible although the same remarks as above regarding realizability apply. It can be seen from (3) that the effect of the disturbance is now dependent on both the feedforward and the feedback controller. Thus, if perfect disturbance rejection is not possible the responses from the open- and the closed loop will differ. With the closed-loop structure, the controllers will interact which might lead to a deterioration in performance compared to the open-loop structure. The remedies for this can be divided into two categories. Firstly, the feedforward controllers can be tuned, taking the feedback controller into account. Ways of modifying the feedforward controller in order to get satisfying response from the closed-loop system has been presented in [7] and [10]. The drawback with these kind of approaches is that if the feedback controller is retuned, the feedforward controller needs to be retuned as well. Secondly, the effect of the interaction can be decreased or even eliminated by yet another feedforward to the feedback controller input, see Fig. 3. The advantage with this method is that the feedforward and the feedback controllers can be tuned individually. A drawback is the increased overall complexity of the controller. A feedforward control structure, equivalent to the one in Fig. 3, that achieves the desired decoupling was presented in [4]. Dropping the argument s, the transfer function from d to y is given by

$$G_{\text{cl}} = \frac{P_d - P_u(F - CH)}{1 + P_u C}. \tag{4}$$

Choosing H as

$$H = P_d - P_u F, \tag{5}$$

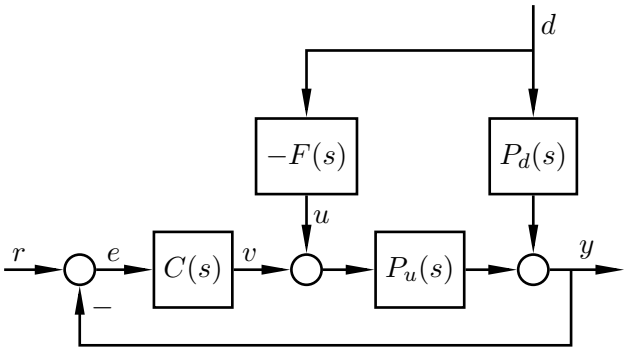

Figure 2: Closed-loop structure commonly used when combining feedforward and feedback control.

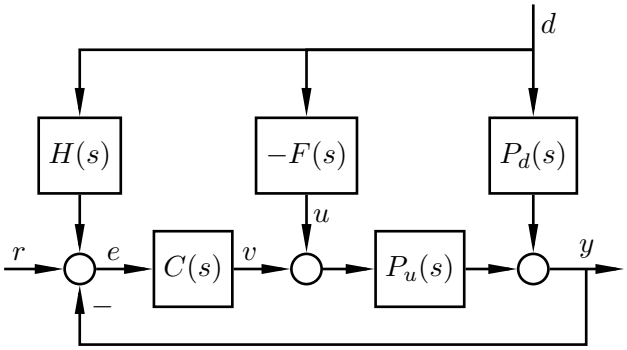

Figure 3: Controller structure that decouples the response, and design, of the feedback and feedforward controllers.

the closed loop transfer function (4) then equals

$$G_{\mathrm{cl}} = P_d - P_u F = G_{\mathrm{o}}.$$

The closed-loop response from a disturbance d will thus be the same as the response in the open-loop case in (1) and the feedback controller, C, will not interact with the feedforward controller, F. By using the structure in Fig. 3 with H chosen as (5) it is possible to design the feedforward controller by just considering the open-loop response from d.

3. Optimal Feedforward Control

Tuning rules for both feedback and feedforward controllers are often based on process models with low complexity, see e.g., [3, 7, 13, 14]. In this section,

feedforward controller parameters will be derived in the same spirit. The parameters will be obtained as the solution to an optimization problem that ensures that the system has good disturbance attenuation.

The considered feedforward controller is a lead-lag filter, or equivalently, a lowpass filtered PD-controller, with possibly a time delay i.e.

$$F(s) = K_{\text{ff}} \frac{1 + sT_z}{1 + sT_p} e^{-sL_{\text{ff}}} \tag{6}$$

with in total four parameters to choose. Deriving simple analytic tuning rules that are optimal for more advanced feedforward controllers are not tractable.

By using the controller structure in Fig. 3, the feedforward controller can be designed for the open-loop case depicted in Fig. 1.

Let the processes P_u and P_d be described by

$$P_u(s) = \frac{K_u}{1 + sT_u} \mathrm{e}^{-sL_u}, \quad P_d(s) = \frac{K_d}{1 + sT_d} \mathrm{e}^{-sL_d}. \tag{7}$$

In the analysis and derivation of optimal controller parameters the disturbance d is assumed to be a unit step. The time response of the system subject to the disturbance can be calculated as $y(t) = \mathcal{L}^{-1}\big(G_{\text{o}}(s)\frac{1}{s}\big)$. The reference signal can without loss of generality be disregarded and for the remainder of this paper r is zero.

The performance is measured by the integrated squared error

$$\text{ISE} = \int_0^\infty e^2(t)\,\mathrm{d}t. \tag{8}$$

A large number of other measures could be considered, cf., [3]. The ISE measure is an established performance measure and is chosen since it enables the derivation of analytical solutions for finding the minimal cost for the setting considered in this paper. The drawbacks of using the ISE as the performance measure is that it penalizes large deviations from the reference hard which gives optimal controllers that may yield large control signals and overshoot in the measured variable.

In the case of $L_u \leq L_d$ perfect feedforward, i.e., no control error, is obtained with the, realizable, controller given by (2). The remainder of this section will therefore focus on the case when $L_u > L_d$ and hence, perfect disturbance rejection is not possible. The time delays in the process models can then, without loss of generality, be shifted so that $L_d = 0$ and the delay in P_u becomes

$$L = L_u - L_d. \tag{9}$$

Optimal feedforward controller parameters that give good disturbance attenuation can be found by solving the nonconvex optimization problem

$$\begin{array}{ll} \underset{K_{\text{ff}},\, L_{\text{ff}},\, T_z,\, T_p}{\text{minimize}} & J = \int_L^\infty y^2(t)\,\mathrm{d}t \\ \text{subject to} & T_p \geq 0 \\ & L_{\text{ff}} \geq 0 \end{array} \tag{10}$$

where the constraints are included to ensure that the controller is stable and causal.

The remainder of this section contains the derivation of the optimal controller parameters. A summary of the result can be found in Sec. 4.

3.1. Optimal Stationary Gain

Using the decoupling structure and provided that the feedback controller has integral action, the steady-state response is $y = r + H(0)d$. It is therefore desirable to ensure that $H(0) = 0$. Furthermore, the integral in (10) converges if and only if the controller's stationary gain is

$$K_{\text{ff}} = \frac{K_d}{K_u}. \tag{11}$$

From (5) it then follows that $H(0) = 0$.

3.2. Feedforward Time Delay

If the time delays are such that perfect disturbance rejection is not possible, the ISE will increase if there is time-delay in the controller. The time delay should therefore be chosen as

$$L_{\text{ff}} = \max(0, -L). \tag{12}$$

3.3. Optimal T_z

Using the optimal static gain (11) and time delay (12) it was shown in [8] that J is a convex quadratic function in the parameter T_z. The expression for J can be found in the Appendix, see (A.1). The unique global minimizer can be found by completion of squares and it is given by

$$T_z^* = (T_u + T_p)\left(1 - \frac{2T_u}{b\,(T_d + T_p)}\right) \tag{13}$$

where

$$a = \frac{T_u}{T_d} \tag{14a}$$

$$b = a\,(a+1)\,\mathrm{e}^{\frac{L}{T_d}}. \tag{14b}$$

Since the optimal choice of T_z is a function of T_p it is not obvious that $T_z^* > 0$, i.e. that the controller will be minimum-phase. That this is in fact the case will be shown in Sec. 5.2.

3.4. Optimal T_p

Denote the cost function evaluated at the optimal K_{ff}, L_{ff} and T_z by

$$\hat{J}(T_p). \tag{15}$$

The expression for $\hat{J}(T_p)$ can be found in the Appendix, see (A.2). The optimal choice of feedforward time constant T_p will either be one of the stationary points of (15) or the boundary point, $T_p = 0$. From an optimization point of view this will be considered to be a feasible solution. This corresponds to the feedforward controller being an ideal PD-controller. The limit as $T_p \to \infty$ is practically the same as no feedforward and will therefore be discarded as a possible solution.

The stationary points to (15) are given as the solutions to

$$\frac{\mathrm{d}\hat{J}}{\mathrm{d}T_p} = 0 \tag{16}$$

and are

$$T_{p_1}^* = \frac{3a - 1 - b + \sqrt{(a-1)^2(1+4b)}}{b-2} T_d \tag{17a}$$

$$T_{p_2}^* = \frac{3a - 1 - b - \sqrt{(a-1)^2(1+4b)}}{b-2} T_d \tag{17b}$$

$$T_{p_3}^* = \frac{2a - b}{b-2} T_d. \tag{17c}$$

Substituting (17c) in (13) gives $T_z^* = T_p^*$, i.e. static feedforward compensation. Define the cost difference between an arbitrary choice of T_p and the boundary controller as

$$D(T_p) = \hat{J}(T_p) - \hat{J}(0). \tag{18}$$

The expression for the cost difference can be found in the Appendix, see (A.4). The static controller gives a higher cost than the PD-controller since

$$D(T_{p_3}^*) = \frac{K_d^2 (b-2a)^2}{2b^2} T_u \geq 0 \tag{19}$$

unless $T_u = T_d$ and $L = 0$ i.e. the scenario where the process dynamics allows for perfect disturbance rejection. Therefore, the stationary point $T_{p_3}^*$ can be excluded as the optimal solution.

3.4.1. Conditions for Nonnegative Stationary Points.

To ensure a stable feedforward controller the time constant T_p must be nonnegative. It was shown in [8] that $T_{p_1}^*$ is nonnegative if and only if

$$a > 1, \qquad b < 4a^2 - 2a \tag{20}$$

and that $T_{p_2}^*$ is nonnegative if and only if

$$a < 1, \qquad b < 2. \tag{21}$$

3.4.2. Simplification of stationary point T_p.

Since $T_{p_1}^*$ and $T_{p_2}^*$ are nonnegative for $a > 1$ and $a < 1$ respectively, the expressions given by (17a) and (17b) can be simplified to the single expression

$$T_p^* = \frac{3a - 1 - b + (a-1)\sqrt{1+4b}}{b-2} T_d. \tag{22}$$

3.4.3. Conditions for Optimal T_p.

The reduced cost function, (15), has three stationary points and approaches infinity when T_p approaches infinity. The cost function can therefore have no more than two local minima. According to (19), $T_{p_3}^*$ renders a higher cost than the boundary $T_p = 0$ and is therefore excluded. Only one of $T_{p_1}^*$ and $T_{p_2}^*$ is positive for any set of process parameters. The optimal solution must therefore be T_p^* or $T_p = 0$.

By determining for which positive T_p that (16) changes its sign, conditions for when T_p^* is optimal can be derived. The difference function can be expressed as

$$D(T_p) = \tilde{K}(T_p)\left(T_p^2 + c_1 T_p + c_0\right) T_p \tag{23}$$

where $\tilde{K}(T_p)$ is positive. The expressions for the $\tilde{K}$, c_1 and c_0 can be found in the Appendix, see (A.5). The positive solution to $D(T_p) = 0$ is

$$T_p = -\frac{c_1}{2} + \sqrt{\frac{c_1^2}{4} - c_0}. \tag{24}$$

Inserting (22) and solving for b gives the following values for which the difference function can change its sign

$$b^* = \begin{cases} 4a^2 - 2a \\ a + \sqrt{a} \\ a - \sqrt{a}. \end{cases} \tag{25}$$

The last of the three solutions can be disregarded since $a - \sqrt{a} < b$ for all values of a and L.

For $a < 1$, the first solution can also be disregarded since $4a^2 - 2a < b$. Furthermore, since

$$\left.\frac{\mathrm{d}D(T_p^*)}{\mathrm{d}b}\right|_{b=a+\sqrt{a}} > 0 \tag{26}$$

the difference function changes sign from negative to positive. The choice of T_p if $a < 1$, is hence,

$$T_p = \begin{cases} T_p^* & \text{if} \quad b < a + \sqrt{a} \\ 0 & \text{if} \quad b \geq a + \sqrt{a}. \end{cases} \tag{27}$$

For $a > 1$, the second solution can be disregarded since $a + \sqrt{a} < b$ and since

$$\left.\frac{\mathrm{d}D(T_p^*)}{\mathrm{d}b}\right|_{b=4a^2-2a} > 0, \tag{28}$$

the sign of the difference function changes from negative to positive for $b = 4a^2 - 2a$. The optimal choice of T_p if $a > 1$ is

$$T_p = \begin{cases} T_p^* & \text{if} \quad b < 4a^2 - 2a \\ 0 & \text{if} \quad b \geq 4a^2 - 2a. \end{cases} \tag{29}$$

The magnitude of the two conditions on b in (27) and (29) are related as

$$4a^2 - 2a < a + \sqrt{a} \Leftrightarrow a < 1. \tag{30}$$

Therefore the optimal choice can be expressed as

$$T_p = \begin{cases} T_p^* & \text{if} \quad b < \begin{cases} 4a^2 - 2a & \text{or} \\ a + \sqrt{a} \end{cases} \\ 0 & \text{otherwise.} \end{cases} \tag{31}$$

3.5. Special cases

There are three parameter combinations that are not treated in the analysis above. The first is the case when $T_d = 0$. In this case, the ISE defined in (8) is equal to

$$J = K_d^2 \frac{T_u^2 + (3\,T_p - 2\,T_z)\,T_u + (T_p - T_z)^2}{2\,(T_u + T_p)}. \tag{32}$$

It can easily be verified that the ISE is zero if the controller parameter are chosen as $T_p = 0$ and $T_z = T_u$.

The second and third overlooked parameter combinations are when the time constants are equal, that is $T_u = T_d$ and subsequently $a = 1$, and when $b = 2$. It has been shown in [8] that the optimal controller parameters are given by $T_p = 0$ and T_z chosen as (13).

4. Design summary

Below follows a summary of how to choose the feedforward controller parameters so that they minimize the ISE and are the solution to the optimization problem formulated in Sec. 3. Calculate the delay difference

$$L = L_u - L_d. \tag{33}$$

If it is negative, perfect disturbance rejection is possible with the controller

$$F = \frac{K_d}{K_u} \frac{1 + sT_u}{1 + sT_d} \mathrm{e}^{-s(L_d - L_u)}. \tag{34}$$

If the delay difference is positive, the optimal ISE controller is obtained by choosing the controller parameters as

1. $K_{\mathrm{ff}} = \dfrac{K_d}{K_u}$.
2. $L_{\mathrm{ff}} = 0$.

3.
   - Calculate $a = T_u/T_d$ and $b = a(a+1)\,\mathrm{e}^{\frac{L}{T_d}}$.
   - If $b < 4a^2 - 2a$ or $b < a + \sqrt{a}$
     $$T_p = \frac{3a - 1 - b + (a-1)\sqrt{1+4b}}{b-2} T_d.$$
   - Otherwise, $T_p = 0$.
4. $$T_z = (T_p + T_u)\left(1 - \frac{2T_u}{b(T_d + T_p)}\right).$$

Note that even though a small T_p can be optimal, it is not necessarily practical or possible to realize such a controller. Considerations related to the controllers noise characteristics and realizability are presented in Sec. 6.

5. Optimal Feedforward Controller Characteristics

This section will provide an illustration of how the optimal controller parameters depend on the process parameters.

5.1. Lead-lag characteristics

The optimal controller will be compared with the commonly used feedforward controller given by (2), where the non-realizable part is discarded i.e.

$$F^0 = \frac{K_d}{K_u}\frac{1 + T_u s}{1 + T_d s}. \tag{35}$$

By not taking the delay difference into account, the time constants alone determine if this controller will have lead or lag characteristics. A feedforward controller will have lead characteristics if $T_z > T_p$ and a lag characteristics if $T_z < T_p$. It is apparent from (35) that this controller switches from a lead- to a lag-filter for $a = 1$. For the optimal controller it is straight-forward, using (13) and (31), to show that $T_z < T_p$ if and only if $a < 1$ and $b < a + \sqrt{a}$. Examples of the optimal controller parameters as functions of the process parameters can be seen in Fig. 4 and Fig. 5. These figures show how the optimal controller parameters depend on the the time-delay difference L. For $L = 0$ it is easily verified, using (14) and (22) that $T_p^* = T_d$. Furthermore, its derivative with respect to L is

$$\frac{\mathrm{d}T_p^*}{\mathrm{d}L} = (1-a)\,\frac{\left(2\,b + 5 + 3\,\sqrt{1+4\,b}\right)b}{\sqrt{1+4\,b}\,(b-2)^2}, \tag{36}$$

from which it, together with (31), can be concluded that $T_p^* > T_d$ if and only if $a < 1$ and $b < \sqrt{a} + a$. This can be seen in Fig. 4 and Fig. 5.

5.2. Nonnegativity of the optimal T_z.

It follows from (13) that T_z^*, is nonnegative if and only if

$$(b - 2a)T_d + bT_p \geq 0. \tag{37}$$

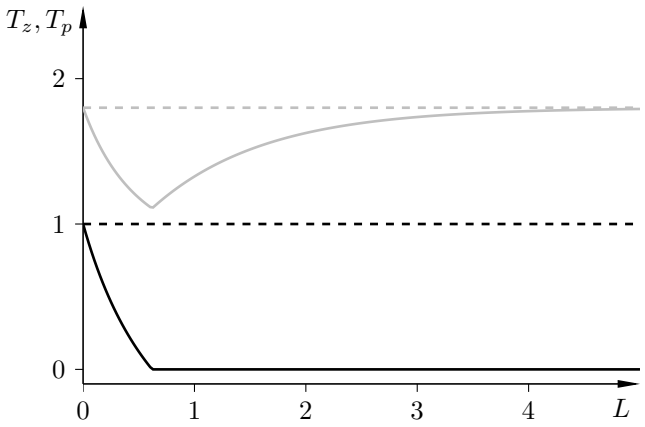

Figure 4: Controller parameters as functions of the delay difference L for $T_u = 1.8$, $T_d = 1$. The solid lines correspond to the optimal controller parameters and the dashed lines correspond to the common controller (35). T_p and T_z in black and gray respectively.

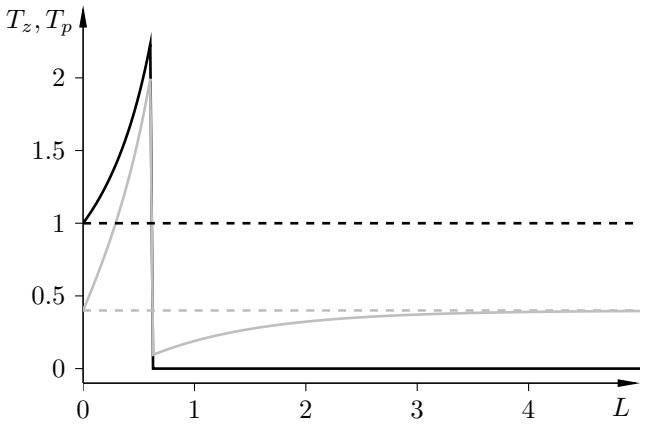

Figure 5: Controller parameters as functions of the delay difference L for $T_u = 0.4$, $T_d = 1$. The full lines correspond to the optimal controller parameters and the dashed lines correspond to the common controller (35). T_p and T_z in black and gray respectively.

Furthermore, from the definition of b (14) it also follows that

$$a \geq 1 \Rightarrow b \geq 2a \tag{38}$$

and thus, the optimal T_z is positive for $a \geq 1$.

For time-constant ratios $a < 1$ and long time delay differences L, the optimal value of T_p is zero according to (31). In this case T_z is nonnegative since

$$b > \sqrt{a} + a > 2a \tag{39}$$

and the inequality (37) is satisfied.

For the last case, $a <$ and $b < \sqrt{a} + a$, the optimal T_z is positive since

$$(b - 2a)T_d + bT_p > a(a + 1)(T_d + T_p) - 2aT_d > 0 \tag{40}$$

where the first inequality follows from the definition of b and that L is positive. The second inequality holds since, $T_p^* > T_d$. Using T_p^* will therefore give an optimal T_z that is positive.

Asymptotic Controller Parameters

If the delay difference L is zero, the expressions for the optimal controller parameters simplify $T_p = T_d$ and $T_z = T_u$ i.e. the controller given by (2) is realizable and the disturbance will not give rise to any control error. The design rules for the optimal controller behaves as expected for $L = 0$. This is also true for the case of very large time-delay difference.

According to the definition of b, (14), and optimal choice of T_p, (31), $T_p = 0$ is optimal if the time-delay difference L is sufficiently large. From (13) it can be shown that

$$\lim_{L \to \infty} T_z = T_u. \tag{41}$$

This means that if the time-delay difference is large no additional lag is introduced by the feedforward controller and the pole in P_u is canceled. This can be seen in the figures 4 and 5.

6. Control signal considerations

The optimal controller proposed minimizes the integrated-squared error but can be sensitive to high-frequency noise and give rise to large control signals. The high-frequency gain of the controller is

$$K_{\text{ff}} \frac{T_z}{T_p} \tag{42}$$

and using the optimal controller parameters can give too large, or even infinite, high-frequency gain. The unit step response of the controller is

$$u(t) = -K_{\text{ff}} \left(1 + \frac{(T_z - T_p)\, \mathrm{e}^{-t/T_p}}{T_p} \right) \tag{43}$$

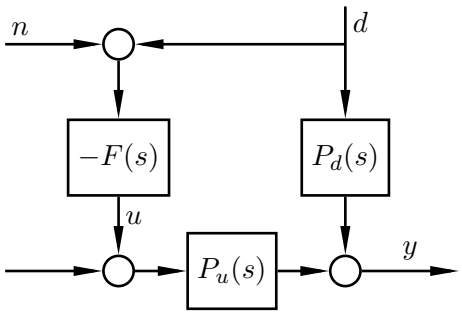

Figure 6: Open-loop structure with measurement noise, n, on the controller input.

from which it can be concluded that the largest magnitude of the signal is equal to the high-frequency gain given by (42). A large ratio between T_z and T_p can be undesirable for two reasons; it yields large control signals and, can amplify and feed measurement noise into the feedback loop.

To limit the effect of high-frequency noise and to get a smoother control signal, the feedforward controller (6) is augmented with a second-order low-pass filter;

$$F_f(s) = K_{\text{ff}} \frac{1 + sT_z}{(1 + sT_p)} \frac{1}{(1 + sT_f)^2} \mathrm{e}^{-sL_{\text{ff}}}. \tag{44}$$

We propose that the parameters K_{ff}, L_{ff}, T_z and T_p are chosen in accordance to what is optimal for a controller such as (6). The filter time constant T_f is then chosen so that the noise propagation through the controller and control signal activity is satisfactory. The order of the low-pass filter is chosen so that the feedforward controller has roll-off also when T_p is zero.

With the added high-frequency roll-off, control action will be smoother and the wear on the actuator will decrease.

Assuming additive white noise corruption, n, on the controller input, see Fig. 6, the variance of controller output is

$$\text{var}\,(u) = \frac{K_{\text{ff}}}{4T_f} \left(1 + \frac{T_z^2 - T_p^2}{(T_f + T_p)^2} \right). \tag{45}$$

This can be shown, using methods from [1], to be equal to

$$\int_0^\infty \left(\frac{\mathrm{d}u(t)}{\mathrm{d}t} \right)^2 \mathrm{d}t \tag{46}$$

which is a measure of the actuator movement during a unit-step disturbance. By increasing T_f, the control signal will be smoother and less aggressive, possibly at the expense of decreased performance.

According to (31), the optimal choice of T_p is zero if b is large which is implied if the delay difference is large. For $T_p = 0$, two approaches to chose T_f

are presented below. Firstly, it will be shown how to choose T_f to limit the peak in the control signal. The tuning rule is derived, as were the ISE-optimal tuning rules, for a unit step-disturbance. Secondly, it will be shown how to choose T_f to limit the peak in the controller's Bode magnitude plot.

High-frequency noise, arising from the measurements of the disturbance, will be attenuated if H is strictly proper. However, if this noise is not sufficiently attenuated by H, the feedback controller should have roll-off to prevent the noise from being amplified and fed into the feedback system. For PID-controllers the necessity of filtering and how the filter should be designed have been treated in [11].

The introduction of the low-pass filter also makes it meaningful to address the problem of noise when perfect feedforward is possible. This will be treated in Sec. 7.

6.1. Filter choice for $T_p = 0$.

The design rules for an optimal lead-lag feedforward controller given in Sec.4 will for long time delays state that T_p is zero. The feedforward controller is then an ideal PD-controller and a special case of (44) given by

$$F_0(s) = K_{\text{ff}} \frac{1 + sT_z}{(1 + sT_f)^2} e^{-sL_{\text{ff}}}. \tag{47}$$

For this controller, considerations regarding the control signal characteristics can be derived without approximations. This is also the worst case scenario from a control signal perspective since

$$|F_0(i\omega)| \geq |F_f(i\omega)|. \tag{48}$$

Limiting the control signal peak

The filter time constant can be chosen such that the control signal peak when the system is subject to a step disturbance is smaller than some user-specified value. The control signal, using (47), subject to a unit-step disturbance is

$$u(t) = -K_{\text{ff}} \left(1 - \frac{T_f^2 - \tau(T_z - T_f)}{T_f^2} \mathrm{e}^{-\frac{\tau}{T_f}} \right) \tag{49}$$

where $\tau = t - L_{\text{ff}}$. Differentiating by, and solving for τ, the control signal peak can be be shown to be obtained at

$$t_{\text{peak}} = \frac{T_z T_f}{T_z - T_f} + L_{\text{ff}}. \tag{50}$$

The peak in the control signal is

$$u(t_{\text{peak}}) = -K_{\text{ff}} \left(1 + \frac{T_z - T_f}{T_f} \mathrm{e}^{\frac{T_z}{T_f - T_z}} \right). \tag{51}$$

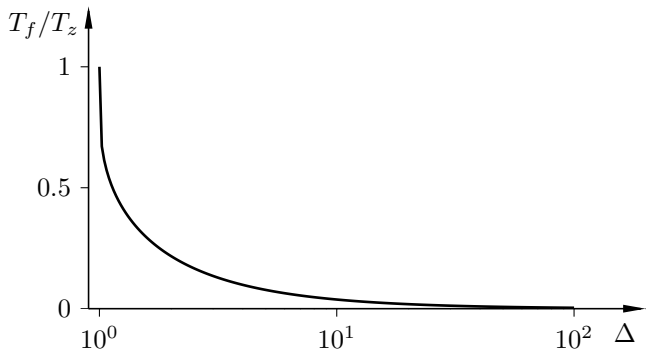

Figure 7: The ratio between T_f and T_z as a function of the desired control signal peak magnitude Δ.

By introducing $x = T_f/(T_z - T_f)$, the expression for the peak being Δ times larger than K_{ff}, can be expressed by

$$u\left(t_{\text{peak}}\right) = -K_{\text{ff}}\left(1 + \frac{1}{x}\mathrm{e}^{-(x+1)}\right) = -K_{\text{ff}}\Delta. \tag{52}$$

The equation can be rewritten as

$$x\mathrm{e}^{x} = \frac{\mathrm{e}^{-1}}{\Delta - 1} \tag{53}$$

for which the solution is given by the Lambert W-function i.e.

$$x = W\left(\frac{\mathrm{e}^{-1}}{\Delta - 1}\right), \quad \Delta > 1. \tag{54}$$

By assumption, Δ is larger than one and the argument to the Lambert W-function is therefore positive and real, and the solution to (53) is therefore given by the principal branch W_0 of the W function. See [5] for an introduction to, a brief history, and computational aspects of the Lambert W-function. To obtain a control signal with a peak Δ the filter time-constant should be chosen as

$$T_f = \frac{T_z}{1 + \frac{1}{W_0\left(\frac{\mathrm{e}^{-1}}{\Delta - 1}\right)}}. \tag{55}$$

The ratio between the filter time-constant and T_z is thus a function of the desired control signal peak magnitude Δ. This function is displayed in Fig. 7. It can be seen in the figure that for example choosing the filter time constant as a fifth of T_z yields a control signal peak approximately twice as large as the static gain.

6.2. Bode magnitude peak reduction

The filter time-constant can also be chosen such that the largest value of the Bode magnitude-plot is equal to or lower than a desired value. The maximum of the Bode magnitude is

$$\gamma_0 = \max_{\omega} |F_0(i\omega)| \tag{56}$$

and the maximum occurs at the frequency

$$\omega^* = \frac{\sqrt{T_z^2 - 2T_f^2}}{T_z T_f}, \tag{57}$$

which means that ω^* is the only positive real solution to

$$\frac{\mathrm{d}F_0(i\omega)}{\mathrm{d}\omega} = 0. \tag{58}$$

The magnitude of the Bode plot peak at the frequency ω^* is

$$\gamma_0 = K_{\mathrm{ff}} \frac{T_z^2}{2T_f\sqrt{T_z^2 - T_f^2}}. \tag{59}$$

Solving this equation for T_f gives

$$T_f = \frac{T_z}{\sqrt{2}}\sqrt{1 - \sqrt{1 - \frac{K_{\mathrm{ff}}^2}{\gamma_0^2}}}, \qquad \gamma_0 > K_{\mathrm{ff}}, \tag{60}$$

which can be used as a design rule to choose the filter time-constant. The condition that γ_0 should be larger than K_{ff} is necessary since if $T_f > T_z/\sqrt{2}$ the maximum will be K_{ff} and occur at $\omega = 0$. Figure 8 shows how the ratio between T_f and T_z depends on the desired Bode peak magnitude.

6.2.1. Filter choice for $T_p > 0$.

For the lead-lag feedforward controller (6), the high-frequency gain (42) is finite if $T_p > 0$ but it can still be too large. If $T_z > T_p$ the high frequency gain will be larger than K_{ff}. Deriving an analytic solution to the problem of limiting the Bode magnitude is not tractable and therefore an approximation is derived and presented in this section.

The magnitude of the controller's Bode plot is

$$|F_f(i\omega, T_f)| = K_{\mathrm{ff}}\sqrt{\frac{1 + \omega^2 T_z^2}{1 + \omega^2 T_p^2}} \cdot \frac{1}{1 + \omega^2 T_f^2}. \tag{61}$$

A necessary condition for the Bode plot to have a peak larger than K_{ff} is that $T_z > T_p$. The peak will be located at the positive real solution to

$$\frac{\mathrm{d}\,|F_f(i\omega, T_f)|}{\mathrm{d}\omega} = 0. \tag{62}$$

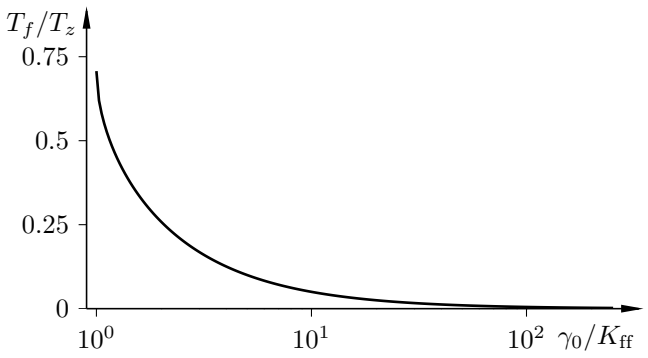

Figure 8: The ratio between T_f and T_z as a function of the desired Bode peak magnitude γ_0/K_{ff}.

Straight-forward but tedious calculations give that a positive real solution exists if and only if

$$0 < T_f < \sqrt{\frac{T_z^2 - T_p^2}{2}} = \hat{T}_f. \tag{63}$$

If noise conditions or constraints on the control signals aggressiveness are such that the filter time constant has to be chosen larger than this upper bound, the benefit of using the optimal parameter values diminishes to a level where a second order low-pass filter should be considered as the feedforward controller.

Denote the peak of the Bode magnitude plot

$$\gamma(T_f) = \max_{\omega} |F_f(i\omega, T_f)| \tag{64}$$

which has the the following boundary conditions

$$\begin{aligned} &\gamma(0) = K_{\text{ff}}\tfrac{T_z}{T_p}, \qquad &&\gamma'(0) = -K_{\text{ff}}\tfrac{2\hat{T}_f}{T_p^2}, \\ &\gamma(\hat{T}_f) = K_{\text{ff}}, \qquad &&\gamma'(\hat{T}_f) = 0. \end{aligned} \tag{65}$$

As an approximation of the peak consider the function

$$\tilde{\gamma} = K_{\text{ff}} \frac{b_1 T_f + b_2}{T_f^2 + b_3 T_f + b_4} \tag{66}$$

where the parameters b_i are determined so that the approximation has the same boundary conditions as (65). This results in

$$\tilde{\gamma} = K_{\text{ff}} \frac{\hat{T}_f T_f + \frac{1}{2} T_z (T_z + T_p)}{T_f^2 - \hat{T}_f T_f + \frac{1}{2} T_p (T_z + T_p)}. \tag{67}$$

Denote the peak magnitude relative to the static gain by λ, i.e. $\lambda = \tilde{\gamma}/K_{\text{ff}}$. By solving (67) for T_f, the filter time-constant can be determined by

$$T_f = \frac{\hat{T}_f(1+\lambda)}{2\lambda} \sqrt{1 - \frac{2\lambda(T_z - \lambda T_p)(T_z + T_p)}{(1+\lambda)^2 \hat{T}_f^2}}. \tag{68}$$

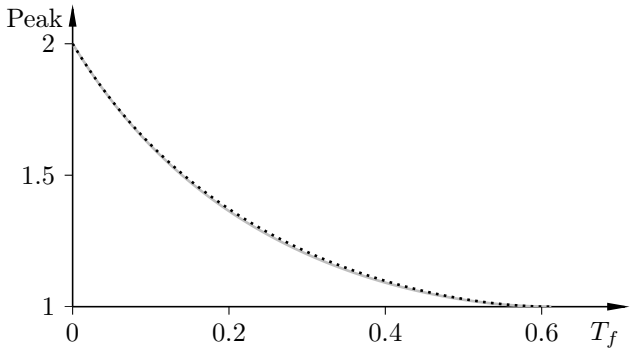

Figure 9: The true Bode peak magnitude (gray) and the approximation (black) given by (68) as functions of the filter time constant T_f. The controller parameters are $K_{\text{ff}} = 1$, $T_z = 1$ and $T_p = 0.5$.

An example of the true Bode magnitude peak and its approximation can be seen in Fig. 9 where $T_z = 1$, $T_p = 0.5$. The approximation is close to the true value of the Bode magnitude peak.

7. Precompensation

Without the noise-reducing filter, perfect disturbance rejection is possible with the controller (2) if $L_u \leq L_d$. However, this controller can suffer from noise sensitivity and aggressive control action. Adding the low-pass filter will reduce these problems but it will also deteriorate the performance.

With the introduction of the low-pass filter to the optimal controller, additional lag is introduced. However, if the optimal controller contains a time delay, this can be adjusted in order to reduce the lag from the filter. Consider the controller (44) with the time delay

$$L_{\text{ff}} = L_d - L_u + \delta \tag{69}$$

where δ denotes the time-delay shift. Denote the integrated-squared error (8) obtained with this controller J_f. This is a convex function of δ since

$$\frac{\mathrm{d}^2 J_f}{\mathrm{d}\delta^2} = \frac{2\,K_d^2 T_d^2\,(T_d + T_z)}{\mathrm{e}^{\frac{\delta}{T_d}}\,(T_p + T_d)\,(T_f + T_d)^2\,(T_u + T_d)} \geq 0$$

and hence the unique minimizer is given by the only stationary point J_f i.e.

$$\delta^* = \ln\left(\frac{2T_d^3\,(T_d + T_z)}{(T_f + T_d)^2 (T_p + T_d)(T_u + T_d)}\right) T_d. \tag{70}$$

By using the T_p and T_z that are optimal in the case without the low-pass filter, this expression simplifies to

$$\delta^* = 2\ln\left(\frac{T_d}{T_f + T_d}\right) T_d. \tag{71}$$

This indicates that the delay in the controller should be decreased when filtering is introduced. The time delay L_{ff} in the controller must be positive and it follows from (69) that

$$\delta \geq L_u - L_d. \tag{72}$$

Hence, there exists a bound on the filter time-constant T_f for which the controller delay will be zero. Introducing (71) into the inequality (72) and solving for the filter time constant gives

$$T_f \leq T_d \left(\mathrm{e}^{\frac{L_d - L_u}{2T_d}} - 1 \right). \tag{73}$$

For reasonable amounts of filtering, the time-delay shift rules provided in (70) and (71) reclaims some of the performance lost by the introduction of the low-pass filter.

8. Design Examples

In this section two examples are presented to illustrate that the ideas presented in this paper also work well in a closed-loop setting where the process models differ from the actual processes. The first examples compares the different control structures as well as makes use of the design considerations from Sec. 6. The last example shows that the concepts of precompensation is an easy way to increasing performance when the closed-loop decoupling structure is used.

Example 1 (Closed-loop performance). This example illustrates how the feedforward structure presented in Fig. 3 and the design rules presented in this paper performs in a setting with noise and uncertain process models . It also shows the benefits of feedforward control and especially feedforward control using the decoupling structure.

Consider the controller structure in Fig. 3 with the processes given by

$$P_u(s) = \tfrac{1}{(1+s)^3}, \qquad P_d(s) = \tfrac{1}{(1+0.1s)^2} \tag{74}$$

and their FOTD-approximations

$$P_u^*(s) = \tfrac{1}{1+2.45s}\mathrm{e}^{-0.81s}, \qquad P_d^*(s) = \tfrac{1}{1+0.19s}\mathrm{e}^{-0.03s}.$$

To simulate a scenario where the process knowledge is limited, the controllers will be designed based on the approximations.

The feedback controller is a PI controller, where the controller parameters are found using the method in [9], given by

$$C(s) = 0.55 + \frac{0.27}{s}. \tag{75}$$

Using the design rules in Sec. 4 yields the, nonrealizable, feedforward controller

$$F^0 = 1 + 2.44s. \tag{76}$$

Table 1: Performance measures for the control strategies in Example 1.

Scenario	ISE	IAE	u_{peak}
FB only	1.75	2.91	1.49
FB and FF	1.30	2.95	5.62
FB, FF and decoupling	0.86	1.91	4.99

To obtain a realizable controller that doesn't suffer from high-frequency noise amplification, a filter is augmented to the feedforward controller. The filter time-constant is chosen so that the control signal peak is $\Delta = 5$ using (55). The feedforward controller with low-pass filter is

$$F = \frac{1 + 2.44s}{(1 + 0.19s)^2}. \tag{77}$$

Assuming that perfect process knowledge is not available, the decoupling filter is based on the approximations i.e.

$$H = P_u^* - P_d^* F. \tag{78}$$

The system is simulated using the processes (74) with band-limited white noise added to the measurements of the disturbance d. The noise power is $5 \cdot 10^{-9}$ and the sample time is 10^{-4} units. The disturbance is a unit-step entering at $t = 1$. In order to compare the performance of the controller and the structures, the results from three simulations can be seen in Fig. 10. The gray curves correspond to pure feedback control, i.e. $F = 0$ and $H = 0$ and are provided for reference. The black dash-dotted curves correspond to feedforward control using the controller (77) with $H = 0$, i.e. no control action decoupling. Finally, the black solid curves correspond to a simulation where both the feedforward controller (77) and the decoupler (78) was used. The measurement noise on the feedforward controller input is effectively attenuated to such a degree that it is not visible in the control signal, Fig. 10. As can be seen from Table 1, the introduction of feedforward action increases the ability to reject the disturbance in measures of ISE but not integrated absolute error, IAE. Although the feedforward controller would perform well in an open-loop setting, in closed-loop the interaction with the feedback controller yields large control signals and a significant undershoot in the disturbance response. The decoupling filter increases performance as well as makes it possible to re-tune either the feedforward and feedback controllers without the need to re-tune the other. The output from the feedback controller can be seen in Fig. 11. Comparing the black curves, it can be concluded that the introduction of the decoupler reduces the control action from the feedback controller. With the decoupling filter, the feedback controller only acts on the mismatch between the model and the process.

Example 2 (Closed-loop performance using precompensation). This example will show that the concept of precompensation works well in a closed-loop

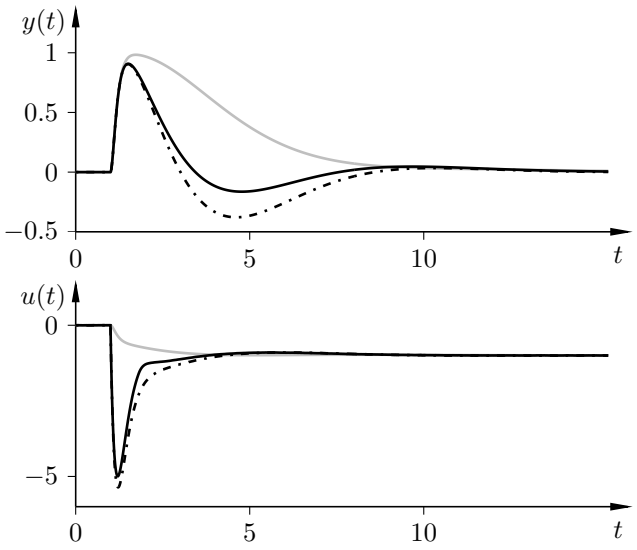

Figure 10: Output (upper) and control signals (lower) for the scenarios in Example 1. The solid gray curves correspond to only feedback control, the dash-dotted black curves to feedback and feedforward control using the conventional controller structure, Fig. 2, and the solid black to feedback and feedforward control using the decoupling structure, Fig. 3.

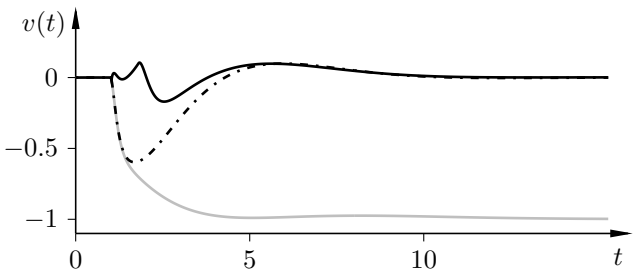

Figure 11: Feedback controller output for the scenarios in Example 1. The solid gray curves correspond to only feedback control, the dash-dotted black curves to feedback and feedforward control using the conventional controller structure, Fig. 2, and the solid black to feedback and feedforward control using the decoupling structure, Fig. 3.

setting where the process' dynamics are not fully known. Consider a system with the structure as in Fig. 3 with the same process dynamics as the Example 1 except for an added time delay of two time units in the disturbance dynamics i.e.

$$P_u(s) = \frac{1}{(1+s)^3}, \qquad P_d(s) = \frac{1}{(1+0.1s)^2}\mathrm{e}^{-2s} \tag{79}$$

with their FOTD-approximations

$$P_u^*(s) = \frac{1}{1+2.45s}\mathrm{e}^{-0.81s}, \qquad P_d^*(s) = \frac{1}{1+0.19s}\mathrm{e}^{-2.03s}.$$

The same feedback controller, (75), that was used in Example 1 can be used since P_u is unchanged. Using the design rules presented in Sec. 4, the feedforward controller is

$$F_0 = \frac{1+2.45s}{1+0.19s}\mathrm{e}^{-1.22s}. \tag{80}$$

The high-frequency gain of this controller is 12.9, which will be the amplification of high-frequency measurement noise. To limit the noise amplification, low-pass filtering is introduced. To limit the largest value of the Bode magnitude to approximately $\lambda = 5$, (68), is used to calculate a suitable filter time-constant as $T_f = 0.22$. The filtered controller is thus given by

$$F_f = \frac{1+2.45s}{(1+0.19s)(1+0.22s)^2}\mathrm{e}^{-1.22s}. \tag{81}$$

To counter-act the additional lag introduced by the low-pass filter, the time delay may be shifted according to (70), i.e. $\delta = -0.27$ the delay-shifted controller is then given by

$$F_\delta = \frac{1+2.45s}{(1+0.19s)(1+0.22s)^2}\mathrm{e}^{-0.94s}. \tag{82}$$

The three controllers were tested in simulation with the same measurement noise as in the previous example with a unit-step disturbance entering at $t = 0$. In each simulation the decoupling filter was chosen according to (5) as

$$H = P_d^* - P_u^* F. \tag{83}$$

The processes used in the simulations are the ones given by (79). The results from the simulations can be seen in Fig. 12 where the gray curves correspond to the nonfiltered controller, the dash-dotted to the filtered and the black solid to the filtered and delay-shifted controller. The performance measures associated with the simulations can be seen in Table 2. Introducing the low-pass filter reduces the noise-amplification significantly as well as the initial peak in the control signal. However, this comes at the expense of lost performance both in terms of ISE and IAE. By shifting the time-delay in the controller, the performance loss can be reduced while the good noise-properties of the filtered controller remain. This example shows that the method of precompensation works well also in scenarios where the process knowledge is limited and feedback is used together with feedforward.

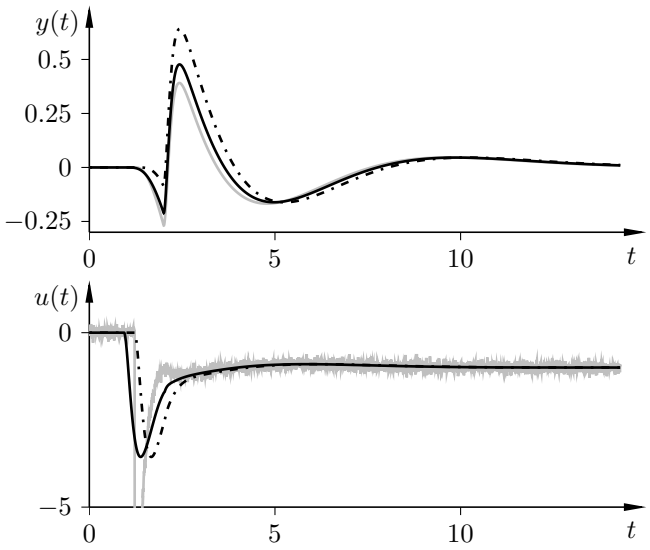

Figure 12: Output (upper) and control signals (lower) using the three controllers presented in Example 2. The gray solid curves correspond to the controller without filtering (80), the dash-dotted black curves to the low-pass filtered controller (81), and the solid black curves to the low-pass filtered controller with precomensation, (82).

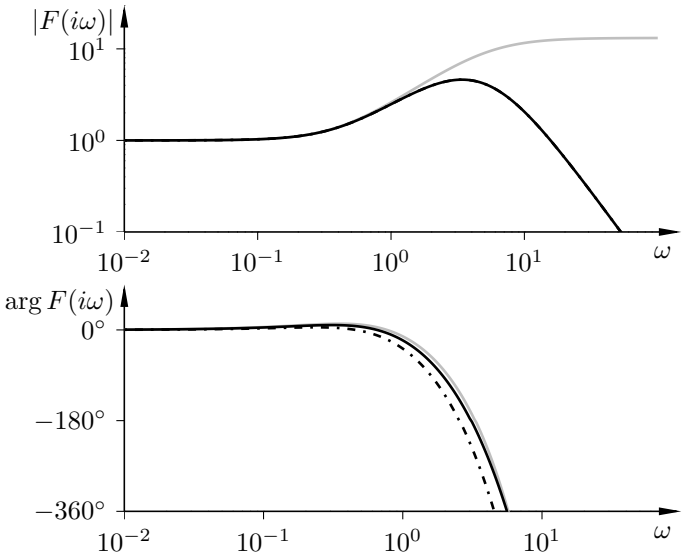

Figure 13: Bode diagram for the three feedforward controllers in Example 2. The gray solid curves correspond to the controller without filtering (80), the dash-dotted black curves to the low-pass filtered controller (81), and the solid black curves to the low-pass filtered controller with precomensation, (82).

Table 2: Performance measures for the control strategies in Example 2.

Controller	ISE	IAE	u_{peak}
$F_0(s)$	0.18	1.13	13.3
$F_f(s)$	0.37	1.38	3.5
$F_\delta(s)$	0.23	1.20	3.5

9. Conclusions

This paper describes how to tune low-order feedforward controllers in order to minimize the integrated squared error for measurable step disturbances. The design rules are derived for an open-loop structure with FOTD plant models. The open-loop controller structure is motivated by the use of a decoupling structure that enables the feedforward and the feedback controllers to be tuned separately. The resulting response to measurable disturbances is that of the open-loop. The paper also describes the characteristics of the optimal controller parameters as functions of the plant model parameters. The optimal feedforward controller can suffer from large high-frequency gain and noise sensitivity which can result in large unwanted control action. To reduce the control action and noise amplification it is proposed that the optimal feedforward controller is low-pass filtered. The filter proposed is a second order filter that assures that the controller has roll-off and thus attenuates high-frequency noise that arises for example from measurement noise.

A number of design methods for choosing the filter time-constant is also proposed. Design rules to limit the peak in both the Bode magnitude or in control signal are provided. Examples show that the controller structure used and the design rules provided gives good performance also in settings with process uncertainties. By filtering the ISE-optimal controllers the control signal characteristics can be significantly improved in terms of variance and aggressiveness with a reasonable loss in performance.

For situations were the disturbance can be completely rejected, design rules for how the time-delay can be shifted in order to compensate low-pass filtering, was provided. This approach of precompensation was shown in examples to give significant performance improvements in open-loop settings in scenarios where filtering of the measurable disturbance was needed. The approach was also tested in simulations in closed-loop with uncertain processes, where it also gave an increase in performance.

10. Acknowledgements

This work was carried out within the framework of the Process Industrial Centre at Lund University (PIC-LU) and supported by the Swedish Foundation for Strategic Research (SSF). The authors are members of the LCCC Linnaeus Center and the eLLIIT Excellence Center at Lund University.

Appendix A. Supplementary Equations

Equations that are related to the analysis of the optimal feedforward controller are presented here for completeness.

With $K_{\text{ff}} = K_d/K_u$ and $L_{\text{ff}} = 0$ the cost function (10) can be expressed as

$$J = \int_L^\infty y^2(t)\,\mathrm{d}t = K_d^2\left(\alpha_2 T_z^2 + \alpha_1 T_z + \alpha_0\right) \tag{A.1}$$

where the coefficients

$$\begin{aligned}
\alpha_0 &= \frac{T_d}{2\mathrm{e}^{\frac{2L}{T_d}}} + \frac{T_p^2+3T_uT_p+T_u^2}{2(T_u+T_p)} - 2a\frac{T_pT_u+T_d(T_p+T_u)}{b(T_p+T_d)} \\
\alpha_1 &= \frac{2T_u}{b(T_p+T_d)} - 1 \\
\alpha_2 &= \frac{1}{2(T_u+T_p)}
\end{aligned}$$

are functions of T_p. The cost function is minimized with respect to T_z by $T_z = -\frac{\alpha_1}{2\alpha_2}$. With this choice of T_z the cost function reduces to

$$\hat{J}(T_p) = K_d^2\left(\alpha_0 - \frac{\alpha_1^2}{4\alpha_2}\right). \tag{A.2}$$

The cost for the boundary controller, $T_p = 0$, is

$$\hat{J}(0) = \frac{K_d^2 a^2\left(a-1\right)^2 T_d}{2b^2}. \tag{A.3}$$

The difference function (18) is given by

$$D(T_p) = \tilde{K}(T_p)\left(T_p^2 + c_1T_p + c_0\right)T_p \tag{A.4}$$

where

$$\begin{aligned}
\tilde{K}(T_p) &= \frac{K_d^2T_u(b-2a)^2}{2b^2(T_u+T_p)(T_p+T_d)^2} \\
c_1 &= \frac{4T_d\left(a^3+(2-b)a^2-(b+1)a+\frac{1}{2}b^2\right)}{(b-2a)^2} \\
c_0 &= \frac{T_d^2\left(8a^3-4a^2+b^2-4a^2b\right)}{(b-2a)^2}.
\end{aligned} \tag{A.5}$$

References

[1] K. J. Åström. *Introduction to Stochastic Control Theory*, volume 70. Academic Press, New York, 1970.

[2] K. J. Åström and T. Hägglund. Revisiting the Ziegler-Nichols step response method for PID control. *Journal of Process Control*, 14(6):635–650, 2004.

[3] K. J. Åström and T. Hägglund. *Advanced PID Control*. ISA, Reasearch Triangle Park, NC, 2005. ISBN 1556179421.

[4] C. Brosilow and B. Joseph. *Techniques of Model-Based Control*. Prentice Hall Professional, 2002. ISBN 013028078X.

[5] R. M. Corless, G. H. Gonnet, D. E. Hare, D. J. Jeffrey, and D. E. Knuth. On the Lambert-W function. *Advances in Computational mathematics*, 5 (1):329–359, 1996.

[6] C. Garcia and M. Morari. Internal model control. A unifying review and some new results. *Industrial & Engineering Chemistry Process Design and Development*, 21(2):308–323, 1982.

[7] J. L. Guzmán and T. Hägglund. Simple tuning rules for feedforward compensators. *Journal of Process Control*, 21(1):92–102, Jan. 2011.

[8] M. Hast and T. Hägglund. Design of optimal low-order feedforward controllers. In *IFAC Conference on Advances in PID Controllers*, Brescia, Italy, 2012.

[9] M. Hast, K. J. Åström, B. Bernhardsson, and S. Boyd. PID design by convex-concave optimization. In *Proceedings European Control Conference*, pages 4460–4465, July 2013.

[10] A. Isaksson, M. Molander, P. Moden, T. Matsko, and K. Starr. Low-order feedforward design optimizing the closed-loop reponse. In *Preprints, Control Systems*, Vanccouver, Canada, 2008.

[11] P. O. Larsson and T. Hägglund. Control signal constraints and filter order selection for PI and PID controllers. In *2011 American Control Conference*, San Francisco, California, USA, June 2011.

[12] A. O'Dwyer. *Handbook of PI and PID controller tuning rules*, volume 2. Imperial College Press London, 2009.

[13] C. Rodríguez, J. L. Guzman, M. Berenguel, and T. Hägglund. Generalized feedforward tuning rules for non-realizable delay inversion. *Journal of Process Control*, 23(9):1241–1250, 2013.

[14] N. J. Sell. *Process control fundamentals for the pulp and paper industry*. Technical Association of the Pulp & Paper Industry, 1995. ISBN 0-899852-294-3.

[15] S. Skogestad. Simple analytic rules for model reduction and PID controller tuning. *Journal of Process Control*, 13(4):291–309, 2003.

[16] R. Vilanova and A. Visioli. *PID Control in the Third Millennium: Lessons Learned and New Approaches*. Springer, 2012.

[17] R. Vilanova, O. Arrieta, and P. Ponsa. IMC based feedforward controller framework for disturbance attenuation on uncertain systems. *ISA Transactions*, 48(4):439–448, 2009.

[18] J. Ziegler and N. Nichols. Optimum settings for automatic controllers. *Transactions of the A.S.M.E*, 5(11):759–768, 1942.